Central European Journal of Energetic Materials
ISSN 1733-7178; e-ISSN 2353-1843

Cent. Eur. J. Energ. Mater. 2025, *22*(4): 470-495; DOI 10.22211/cejem/215879
Article and Supplementary Information is available in PDF-format, in colour, at:
https://ipo.lukasiewicz.gov.pl/wydawnictwa/cejem-woluminy/vol-22-nr-4/

Research paper

1,3,6,8-Tetranitrocarbazole (TNC): Efficient One-Pot Synthesis, X-ray Crystallographic Analysis, and Property Evaluation

Jonas Šarlauskas[1,*], **Mantas Jonušis**[2], **Simona Jonušienė**[2], **Narimantas Čėnas**[1], **Kastis Krikštopaitis**[1], **Jonita Stankevičiūtė**[3], **Žilvinas Anusevičius**[1]

[1] *Vilnius University, Life Sciences Center, Institute of Biochemistry, Department of Xenobiotics Biochemistry, Saulėtekio 7, LT-10257 Vilnius, Lithuania*

[2] *Vilnius University, Life Sciences Center, Institute of Biochemistry, Laboratory of Chemistry of Bioorganic Compounds, Mokslininkų 12A, LT-08412 Vilnius, Lithuania*

[3] *Vilnius University, Life Sciences Center, Institute of Biochemistry, Department of Molecular Microbiology and Biotechnology, Saulėtekio 7, LT-10257 Vilnius, Lithuania*

* *E-mail:* jonas.sarlauskas@bchi.vu.lt

ORCID Information:
Jonas Šarlauskas: https://orcid.org/0000-0003-4268-1716

Abstract: Nitro-substituted derivatives of carbazole represent an important class of compounds with numerous industrial applications, including their role as components of energetic materials. A systematic review of the literature revealed that an effective, practical synthesis method for producing tetranitrocarbazole (TNC) remains elusive. In the present work, we report the development of a new and efficient one-pot nitration procedure utilizing potassium nitrate in fuming sulphuric acid (oleum). This nitration system, comprising potassium nitrate in

oleum (20% SO_3), was found to be significantly more effective for the synthesis of 1,3,6,8-tetranitro-9*H*-carbazole (1,3,6,8-TNC) ($C_{12}H_5N_5O_8$) than the conventional nitration utilizing fuming nitric acid. A monocrystal of pure 1,3,6,8-TNC was used for the detailed X-ray structure determination. It was found that TNC crystallizes in the monoclinic crystal system, space group P21/c, specific crystal density: 1.765 (calc. from X-ray analysis, at –100 °C) or 1.73 g/cm^3 (at 20 °C, by pycnometry). The main properties of TNC are: formula weight: 347.21; melting point: 296 °C; flash point: 350 °C. 1,3,6,8-TNC can be used in various applications in millitary practice, including pyrotechnic compositions and formulations of some specific secondary explosives. The electron-accepting ability and quantum mechanical properties of TNC closely resemble those of tetryl. Its overall explosive properties are expected to be close to those of TNT and picramide.

Keywords: energetic materials, 1,3,6,8-tetranitrocarbazole, synthesis, HPLC-MS analysis, X-ray diffraction

Supplemantary Information (SI):

The SI contains TNC crystal H-bonds description, bond lengths and selected angles in the TNC molecule.

1 Introduction

Carbazole is a tricyclic aromatic heterocycle composed of two benzene rings fused on either side of a five-membered nitrogen-containing ring (Figure 1). Various synthetic procedures for this compound have been developed over the years, but its primary industrial source remains the isolation from coal tar [1]. The recovery of this compound from coal tar distillates is a well-established and cost-effective process, which continues to be favoured due to its simplicity, high yield, and the production of material with high purity. Originally described by Graebe and Glaser in 1872 [2], this method has experienced only minor modifications over time and continues to serve as a fundamental technique for carbazole production, offering consistent efficiency, purity, and cost-effectiveness [3]. Distillation of coal tar within the boiling range of 300-360 °C yields anthracene oil, which, upon cooling and standing, deposits a solid anthracene fraction. This solid is typically separated by filtration and consists primarily of anthracene, carbazole, phenanthrene, and acridine, in varying proportions. The carbazole content within this fraction can range from 5% to 20% by weight, depending on the source and composition of the coal. Purification of carbazole from the crude mixture is typically achieved through selective extraction using organic solvents, followed by fractional crystallization to obtain the compound in high purity.

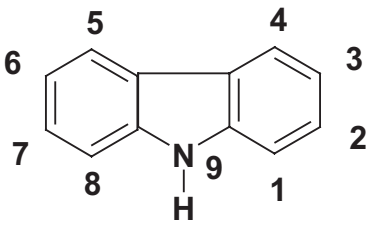

Figure 1. Numbering order in the carbazole molecule

Carbazole is an industrially significant heterocycle, widely utilized in the synthesis of dyes, fungicides, and also used in the manufacture of certain polymers, such as poly(9-vinylcarbazole) (PVK) [1]. Due to their intrinsic electron-donating properties, strong photoconductivity, and nonlinear optical behaviour, carbazole derivatives have also attracted considerable interest in electronic and photonic applications [6, 7]. Furthermore, these compounds exhibit a broad range of biologically relevant activities, including antibacterial [8-10], antitubercular [11], anti-inflammatory [12], and anticancer effects [13-15], making them promising scaffolds in medicinal chemistry and drug development.

Moreover, nitro-substituted derivatives of carbazole represent an important class of compounds with wide-ranging applications in the chemical industry and as components of energetic materials [16-21]. Among these, 1,3,6,8-tetranitro-9*H*-carbazole (1,3,6,8-TNC) is considered the most prominent polynitrated derivative. During World War II, this compound was employed under the name *Gelbmehl* in combustible mixtures for use in time-delay fuses [22]. Today, 1,3,6,8-TNC remains relevant in modern ordnance, where it is utilized in energetic formulations and propellant compositions.

In military practice, 1,3,6,8-TNC has been employed in various pyrotechnic compositions, particularly in formulations for illumination and ignition devices [23-31]. Beyond primary energetic roles, 1,3,6,8-TNC serves as an effective desensitizing agent in formulations containing highly sensitive nitramines, such as 1,3,5-trinitro-1,3,5-triazinane (RDX, hexogen) and 1,3,5,7-tetranitro-1,3,5,7-tetrazocane (HMX, octogen). When added to these formulations, TNC helps to significantly reduce the sensitivity to mechanical stimuli, such as impact, friction, and electrostatic discharge, thereby enhancing the safety profile of the final energetic composition [32].

The present paper focuses on nitro derivatives of carbazole, with particular emphasis on the polynitro derivative 1,3,6,8-TNC, due to its increasing relevance as an energetic material in various formulations [24, 29, 30]. The present study investigated experimentally two distinct nitration methods, aimed at optimizing

a one-pot synthesis of 1,3,6,8-TNC. Additionally, the crystal structure of TNC was elucidated through single-crystal X-ray diffraction analysis, and a set of physicochemical properties of this compound were characterized using experimental and computational methods.

2 Experimental Part

2.1 Materials and test methods

All chemical reagents used for synthesis in this study were from Sigma-Aldrich (Burlington, MA, US).

The melting points of the synthesized nitrocarbazoles were determined using the open capillary method. The purity of the compounds was monitored by TLC, using silica gel 60 F254 aluminium plates (Merck), and by LC-MS analysis using a Shimadzu 2020. UV-VIS spectra of the compounds were recorded using a Perkin-Elmer Lambda 25 UV-VIS spectrophotometer. IR spectra were recorded as KBr discs on a Perkin-Elmer spectrophotometer (FT-IR Spectrum BX II). NMR spectra were recorded using a Varian Unity Inova (400 MHz for ^{1}H NMR). For X-ray analysis a Bruker-Nonius' diffractometer with a KappaCCD detector was used. Diffraction radiation source: fine focus sealed tube; radiation monochromator: graphite. In the crystal structures hydrogen atoms were located and refined. Thermal analysis was investigated using a differential scanning calorimeter Perkin Elmer DSC 8000. Density measurements were performed at 293 K using an AccuPyc 1330 Pycnometer (Micromeritics).

Cyclic voltammetry (CV) was carried out using a standard three-electrode system, consisting of a glassy carbon working electrode (surface area: 0.1 cm^2), an Ag/AgCl reference electrode, and a platinum wire counter electrode. Measurements were conducted using a computer-controlled potentiostat/galvanostat (Parstat 2273, Princeton Applied Research). The CV data were analyzed using the PowerSuite software package.

2.2 Computational details

2.2.1 General

All quantum mechanical computations were carried out using a PC Spartan 10 package (Wavefunction Inc., version 1.1.0, 2011, Irvine, CA, USA). Initial geometry optimization was performed by semi-empirical PM6 Hamiltonian, followed by full optimization at the B3LYP/cc-PVDZ level of theory, without imposing symmetry constraints. The electrostatic potential surface (ESP), frontier

molecular orbitals (FMOs), as well as their corresponding energies, were analyzed at the same level of theory.

2.2.2 Assesment of DFT-based global and local reactivity indices

The DFT-based global reactivity indices of TNC, *i.e.* the chemical hardness (η), chemical softness (S), chemical potential (μ), electronegativity (χ) and the absolute electrophilicity index (ω) were defined based on Koopmans' approximation, in terms of the energies of the highest occupied molecular orbital (E_{HOMO}, as the vertical ionization potential, IP = $-E_{HOMO}$) and the lowest unoccupied molecular orbital (E_{LUMO}, as the vertical electron affinity, EA = $-E_{LUMO}$), according to the following expressions [33, 34]:

$$\eta = 1/S = (E_{LUMO}\text{-}E_{HOMO}),\ \mu = -\chi = (E_{HOMO}+E_{LUMO})/2$$
$$\omega = \mu^2/(2\eta) = (\mu^2/2)S \quad (1)$$

The local electrophilic and nucleophilic regions of the compound were analyzed at the B3LYP/cc-pVDZ level of theory. Local reactivity indices were evaluated in terms of the nucleophilic (P_k^-) and electrophilic (P_k^+) Parr functions, used as substitutes for the Fukui functions [35]. These values were derived from the Mulliken atomic spin densities (ASD) of the radical anion and radical cation species, obtained via single-point energy calculations using the unrestricted UB3LYP formalism (UB3LYP/cc-pVDZ) based on geometries optimized for the neutral state of the compound [35].

2.2.3 Assessment of bond dissociation energies (BDEs)

For assessment of the C–NO_2 bond stability of TNC, BDEs for a homolytic cleavage reaction of the type R–NO_2 → R• + NO_2• were calculated. BDEs were determined as the difference in electronic energies between the parent molecule and its corresponding neutral radical fragments, according to the expression:

$$BDE = E(R\bullet) + E(NO_2\bullet) - E(R\text{–}NO_2) \quad (2)$$

To account for vibrational contributions, the BDEs were further corrected for zero-point energy (ZPE):

$$BDE_{ZPE} = BDE + \Delta ZPE \quad (3)$$

These calculations were performed at the B3LYP/6-31G(d) level, which has been applied for the BDE computation of a wide range of polynitro energetic

materials [36], allowing comparison of the BDEs obtained for TNC with those reported for other polynitro explosive materials.

2.3 Carbazole nitration conditions and products

Mono- and dinitro derivatives of carbazole are well-documented in the literature [37-46]. Under mild nitration conditions, such as treatment with equimolar HNO_3 in nitrobenzene, or nitrating with urea nitrate, carbazole undergoes regioselective nitration predominantly at the 3-position (Figure 1), yielding 3-nitrocarbazole [41, 44, 47-49]. The NH moiety of the fused pyrrole ring in carbazole acts as an electron-donating group *via* both resonance and inductive effects, thereby enhancing the reactivity of the aromatic system, particularly at the C-3 and C-6 positions of the fused benzene rings, towards electrophilic substitution. As shown in Figure 2(a), the nucleophilic regions, characterized in terms of the absolute HOMO density distribution (|HOMO| map) and the nucleophilic Parr function (P_k^-) values, clearly indicate that the C-3 and C-6 positions are the most nucleophilic centers, well aligning with their preferential reactivity in nitration.

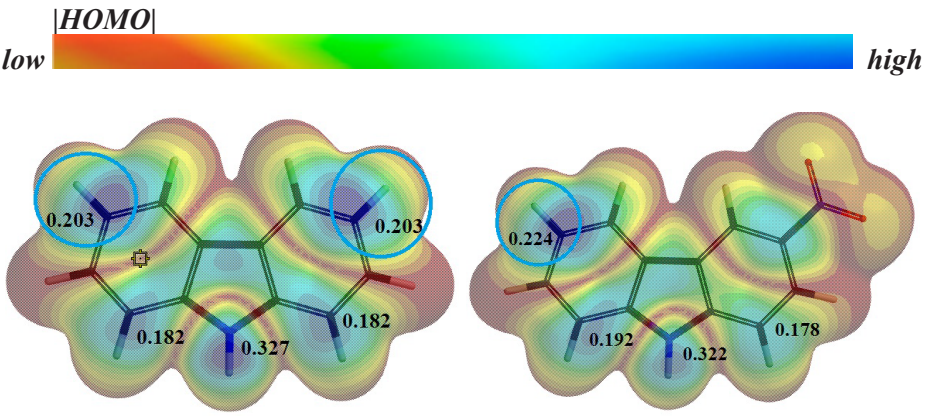

(a) (b)

Figure 2. Absolute HOMO density (|HOMO|, isovalue = 0.004 $Bohr^{-3/2}$) maps and nucleophilic Parr function (Pk^-) values for (a) carbazole and (b) 3-nitrocarbazole (*Note:* HOMO densities were calculated at the RB3LYP/cc-pVDZ level for the neutral species; Pk^- values were derived from atomic spin densities of the corresponding cation radicals at the UB3LYP/cc-pVDZ level, using geometries optimized for the neutral forms)

Similarly, alternative mild nitrating agents, such as tetranitromethane, also exhibit a strong preference for substitution at the C-3 position. For instance, the reaction of 0.25 M tetranitromethane with 0.25 M *N*-ethylcarbazole proceeds slowly in both acetic acid and dichloromethane, yet affords exclusively 3-nitro-*N*-ethylcarbazole (m.p. 126-127 °C) in 90% isolated yield after 30 days at room temperature [50].

Further nitration of 3-nitrocarbazole with excess nitric acid in acetic acid yields two dinitro isomers: 3,6-dinitrocarbazole (major) and 1,6-dinitrocarbazole (minor) [37, 42, 48, 51]. This regioselectivity can also be rationalized based on the distribution of nucleophilic sites in 3-nitro-carbazole, as illustrated in Figure 2(b), showing that the highest nucleophilic center resides at C-6 position, with a P_k^- function value higher than in unsubstituted carbazole, while the local nucleophilicity at the C-1 position, due to the nitro group at C-3, becomes markedly lower.

Subsequent nitration of 3,6-dinitrocarbazole under carefully controlled conditions using a mixture of concentrated H_2SO_4 and HNO_3, with a 20% molar excess of nitric acid, led to the formation of 1,3,6-trinitrocarbazole [18, 51].

Murphy *et al.* [52] in 1953 nitrated carbazole with a HNO_3/H_2SO_4 mixture at increased temperature (60-80 °C) and proposed the separation of two TNC isomers: 1,2,6,8-tetranitrocarbazole (1,2,6,8-TNC), identified as the minor component and 1,3,6,8-TNC, as the major component [52]. However, the structural assignment of these isomers was based solely on IR spectroscopic data and a single chemical characteristic, *viz.* the selective solubility of the unsymmetrical isomer in sodium sulfite solution, which suggested its enhanced reactivity. Given the limitations of these early analytical techniques, the structural identification remains uncertain.

In the study reported herein we have attempted to improve the yield of TNC synthesis and achieve unambiguous identification of both the major and the minor nitration products, including trace-level components, through the application of high-performance liquid chromatography coupled with mass spectrometry (HPLC-MS). The overall nitration pathway and the identified structures of the reaction products are provided in the following schematic representation (Figure 3).

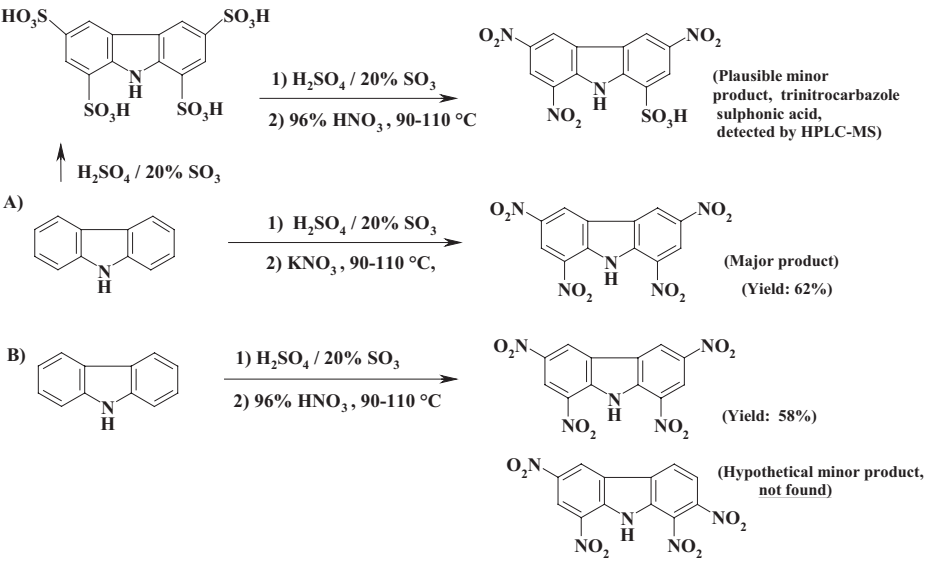

Figure 3. Principal scheme of carbazole nitration reactions and the identified products

3 Procedures Applied for TNC Synthesis

3.1 Method A

A flat-bottom flask was charged with fuming sulfuric acid (oleum, 20% SO_3, 100 mL) and cooled in an ice–water bath to maintain a temperature of approximately 5-10 °C. Carbazole (15 g, 0.09 mol) was then added portionwise to the sulfuric acid under continuous stirring with a magnetic stirrer. The reaction mixture was allowed to gradually warm to 40-60 °C. Once the addition was complete, the resulting brownish reaction mixture was stirred and maintained at 95-100 °C for an additional 3 h to ensure completion of the sulfonation process. The mixture was then allowed to cool to approximately 60 °C. Subsequently, powdered potassium nitrate (46 g, 0.45 mol) was added gradually in small portions, with careful temperature control to ensure that the reaction temperature did not exceed 90 °C during the nitration step. After the complete addition of potassium nitrate, the reaction mixture was maintained at 95-100 °C for an additional 4 h to ensure completion of the nitration. The mixture was then allowed to cool slowly to room temperature with continuous stirring to prevent excessive flotation and accumulation of the precipitated light yellow solid in the center of the vessel.

Finally, the reaction mixture was poured onto crushed ice, resulting in the

formation of a precipitate, which was collected by vacuum filtration. The solid was washed thoroughly with a 1:1 mixture of cold water and acetone to remove residual acids and impurities. The resulting light yellow solid was air-dried to afford 1,3,6,8-TNC as the major product (yield: 19 g, 62%).

The purity of the product, as determined by HPLC analysis, was approximately 96%. Recrystallization from a nitrobenzene/benzene mixture (1:10, v/v) yielded well-formed yellow crystals of a nitrobenzene solvate of TNC. Upon drying at 100 °C in a fume hood overnight, the solvate was converted to a fine white powder of pure TNC, with a melting point of 296 °C.

Other metal nitrates were also evaluated as nitrating reagents in this procedure, including ammonium nitrate, sodium nitrate, and lithium nitrate. These salts, however, did not offer advantages over potassium nitrate, resulting in lower TNC yields and exhibiting undesirable properties such as hygroscopicity.

IR (KBr): 3438, 3091, 1826, 1654, 1618, 1597, 1551, 1541, 1484, 1424, 1394, 1374, 1327, 1292, 1251, 1204, 1128, 1077, 1063, 991, 933, 918, 856, 836, 795, 769, 744, 738, 713, 676, 665, 644, 619, 544, 518, 469, 453 cm^{-1}. (Full spectrum is shown in Figure 4).

UV_{max} = 292, 332 nm.

NMR ^1H spectrum (d_6-DMSO, freq.- 400MHz): 11.95 (s, 1H, 9-NH). 10.00 (s. 2H; 4H- and 5-H) 9.09 (s, 2H; 2-H- and 7-H).

The HRMS (ESI) was calculated for $C_{27}H_{25}N_2O_2$ $[M + H]^+$ 409.19159; found 409.19100.

HPLC-MS (EI, m/z): 346 $[M-H]^-$. HPLC-MS analysis is shown in in Figure 5, Section 3.3.

Interestingly, the TNC obtained *via* Method A was free from analytically detectable impurities, such as the trinitro- or other nitro-carbazole derivatives. Notably, the isomeric form 1,2,6,8-TNC was not observed, even in trace amounts, as confirmed by HPLC-MS analysis.

3.2 Method B

The synthesis of 1,3,6,8-TNC was performed under different one-pot conditions. In the first step, carbazole (10 g, 0.06 mol) was sulfonated with oleum (containing 20% free SO_3, 50 mL) under conditions similar to those described in Method A.

The resulting clear light brown solution at 50 °C was then carefully nitrated by the dropwise addition of precooled 96% HNO_3 (20 mL). Due to the exothermic nature of the reaction, external cooling using a water–ice bath was employed to maintain the temperature. Upon completion of the addition of nitric acid (cooled in a refrigerator at –18 °C), the cooling bath was removed, and the reaction mixture was subsequently heated to 100 ±5 °C and maintained at this temperature

for 3 h. The mixture was then allowed to cool slowly to room temperature.

The reaction product was filtered off using a sintered glass funnel and washed twice with 70% HNO_3 (precooled in a refrigerator at –18 °C), followed by repeated washing with cold distilled water to remove residual acid. The raw product obtained by Method B, when analyzed prior to recrystallization, was found to contain minor traces (2-4%) of a specific impurity: trinitrocarbazole sulfonic acid.

The HPLC-MS analysis of the crude 1,3,6,8-TNC product obtained by Method B is shown in Figure 6. The majority of the sulfonated impurity can be effectively removed by additional washing with cold nitric acid. Subsequent recrystallization from acetic acid yielded pure 1,3,6,8-TNC, as yellowish microcrystals with a melting point of 295-296 °C. The isolated yield was 12 g (58%). The product obtained *via* Method B is considered sufficiently pure for most practical applications.

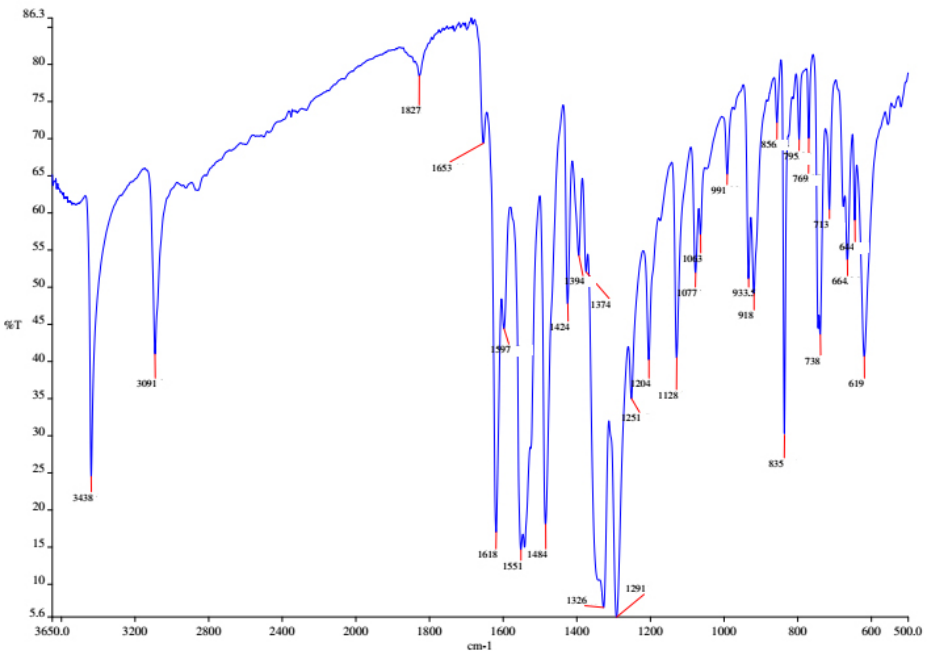

Figure 4. FT-IR spectrum of purified and recrystallized 1,3,6,8-TNC; key absorption bands: 3438 cm^{-1} (N–H stretching), 3091 cm^{-1} (=C–H stretching at positions 2, 4, 5, and 7), 1551 cm^{-1} (symmetric stretching of $–NO_2$ groups), and 1327 cm^{-1} (asymmetric $–NO_2$ stretching)

3.3 LC-MS analysis data of the recrystallized nitration reaction product, 1,3,6,8-TNC (obtained from Method A)

LC-MS analysis of the recrystallized nitration product, 1,3,6,8-TNC, obtained *via* Method A, is shown in Figure 5. The product was recrystallized from a 1:1 nitrobenzene/benzene mixture and dried at 100 °C for 12 h. Notably, TNC obtained by Method A showed no detectable trinitro- or pentanitroderivatives as impurities.

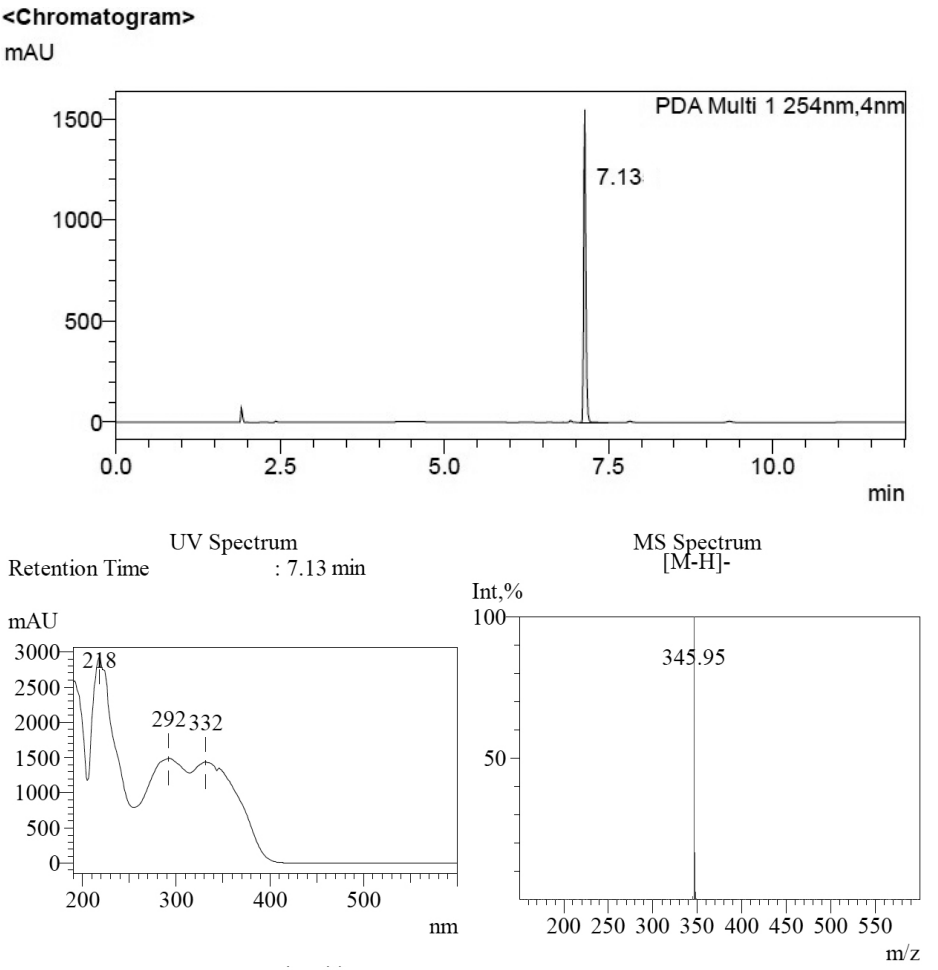

Figure 5. LC-MS analysis of the purified 1,3,6,8-TNC sample obtained *via* Method A

3.4 LC-MS analysis data of recrystallized nitration reaction product, 1,3,6,8-TNC (obtained from Method B)

LC-MS analysis of the raw nitration product 1,3,6,8-TNC, obtained *via* Method B, is shown in Figures 6 (major product) and 7 (minor product). HPLC-MS analysis detected minor amounts of a trinitrocarbazole sulfonic acid as an impurity in the raw product.

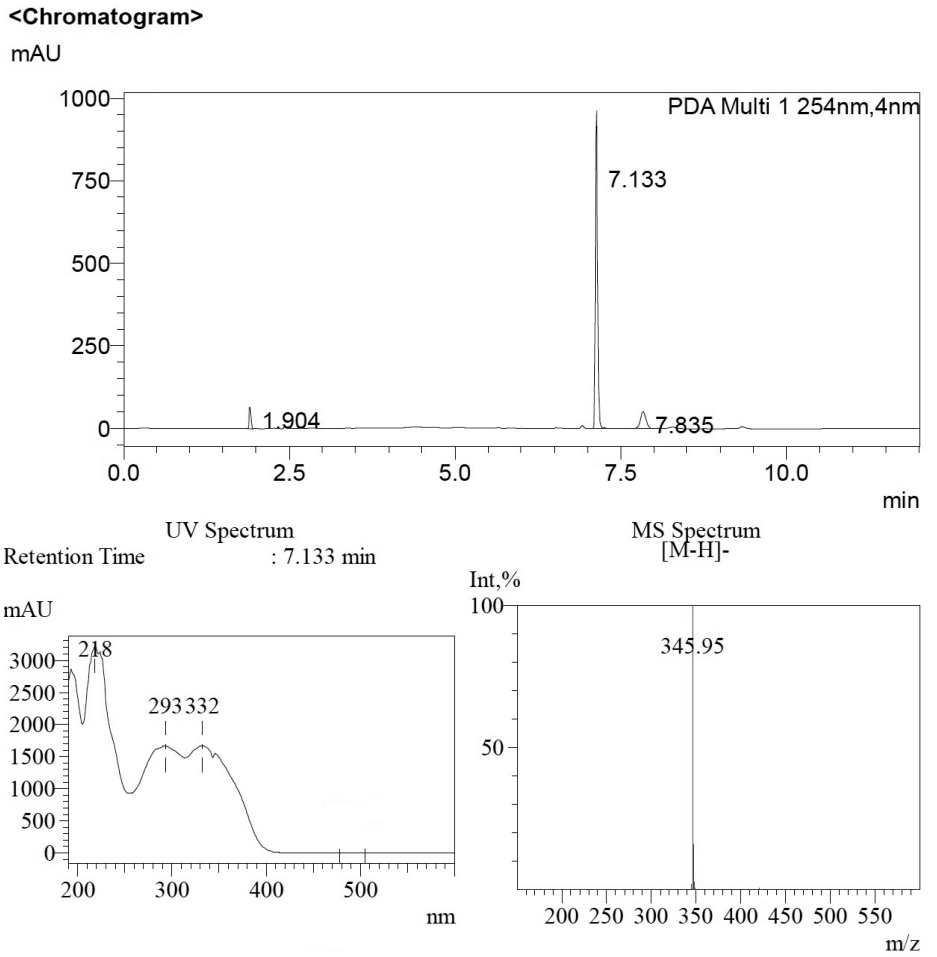

Figure 6. LC-MS analysis data of the raw nitration reaction product TNC (main peak at R.T.= 7.133 min)

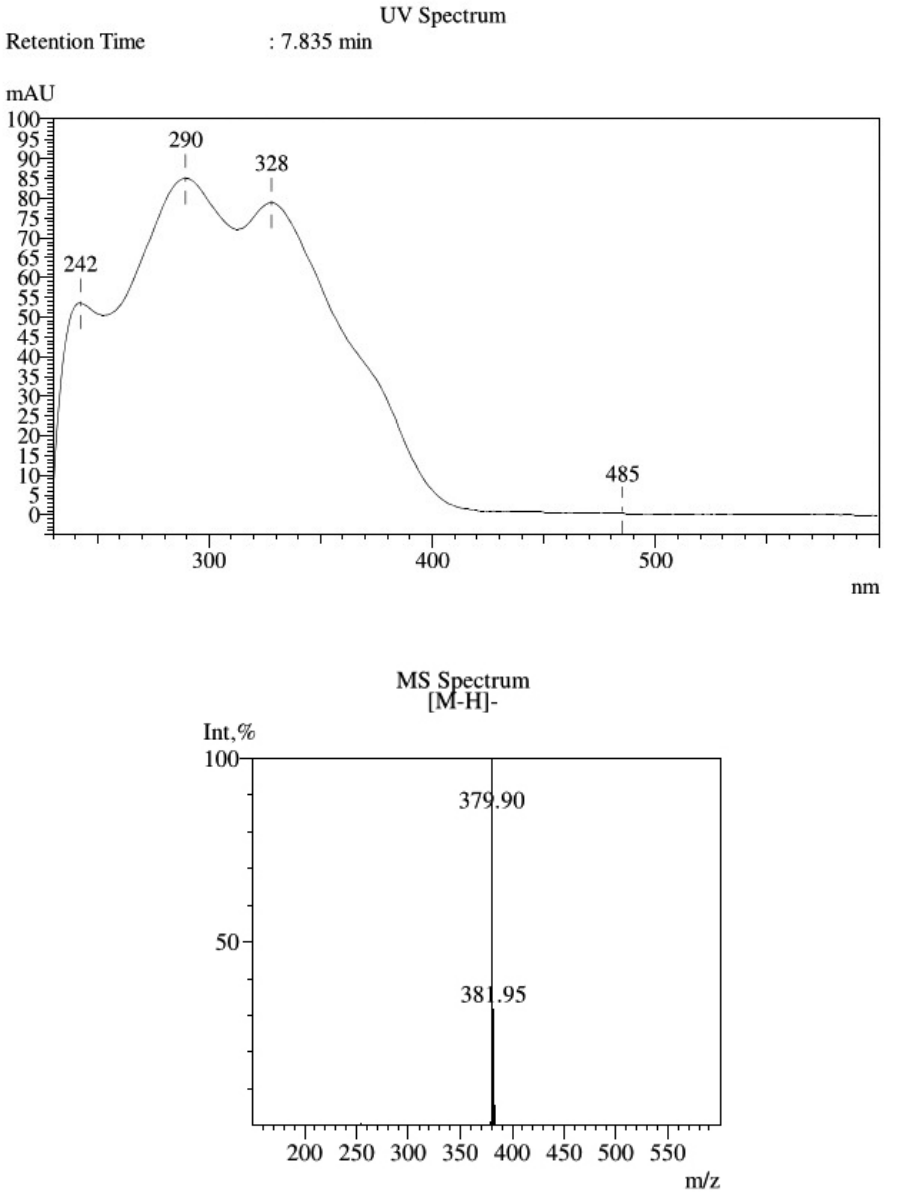

Figure 7. LC-MS analysis of the raw 1,3,6,8-TNC sample obtained *via* Method B, showing a minor by-product identified as a trinitrocarbazole sulfonic acid, observed at a retention time (R.T.) of 7.835 min

3.5 X-ray structure determination of 1,3,6,8-TNC monocrystal

A monocrystal of pure 1,3,6,8-TNC (melting point 296 °C) was grown from a solution in dry nitromethane at 17 °C (room temperature) and was subsequently used for detailed single-crystal X-ray diffraction analysis. Selected crystallographic parameters and refinement details are summarized in Table 1 and in Supplementary Information.

Table 1. Selected crystallographic data and refinement parameters for the X-ray structure determination of TNC

Formula	$C_{12}H_5N_5O_8$
Form. weight [g mol^{-1}]	347.21
Crystal system	monoclinic
Space group	P 21/c
Colour/ Shape	light brown plates from $MeNO_2$
Size [mm]	0.21×0.17×0.04
a [Å]	7.3465(3)
b [Å]	15.0876(7)
c [Å]	12.3372(5)
α [°]	90
β [°]	107.146(3)
γ [°]	90
V [Å^3]	1306.7(1)
Z	4
ρ [g/cm^3]	1.765 (calc. from X-ray analysis); 1.73 (measured by pycnometry)
μ [mm^{-1}]	0.153
F(000)	704
$\lambda_{MoK\alpha}$ [Å]	0.71073
T [K]	173 (2)
Dataset	–9:9, –18:20, –16:16
Reflections collected	5759
Independent reflections	3357
Parameters	230
R_1(obs)	0.0625
wR_2 (all data)	0.1499
GooF	1.037
Largest diff. peak and hole	0.282 and –0.254 e·Å^{-3}
Device type	‚Bruker-Nonius KappaCCD‘
Solution	SHELXS-97
Refinement	SHELXL-97
Absorbtion correction	none

3.5.1 Crystal structure of 1,3,6,8-TNC

An ORTEP representation of the 1,3,6,8-TNC molecular structure is shown in Figure 8, where atomic displacement parameters as thermal ellipsoids are shown at the 50% probability level.

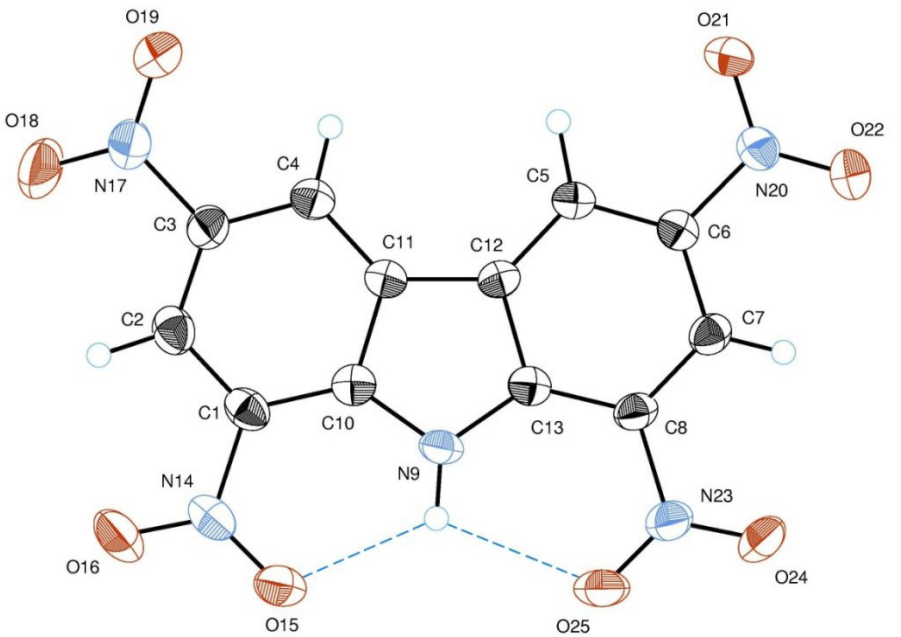

Figure 8. General ORTEP representation of the TNC molecule (Cambridge Crystallographic Data Centre entry: CCDC 1526274)

3.5.2 The single crystal unit cell characterization

As shown in Figure 9, the 1,3,6,8-TNC crystal cell packing is characterized by a wide net of hydrogen bonding which is involved in the compact and dense crystal structure. In its crystal unit cell, dimers of TNC molecules are disposed at specific angles. Additional data about hydrogen bonding, bond lengths and disposition angles may be found in Supplementary Information.

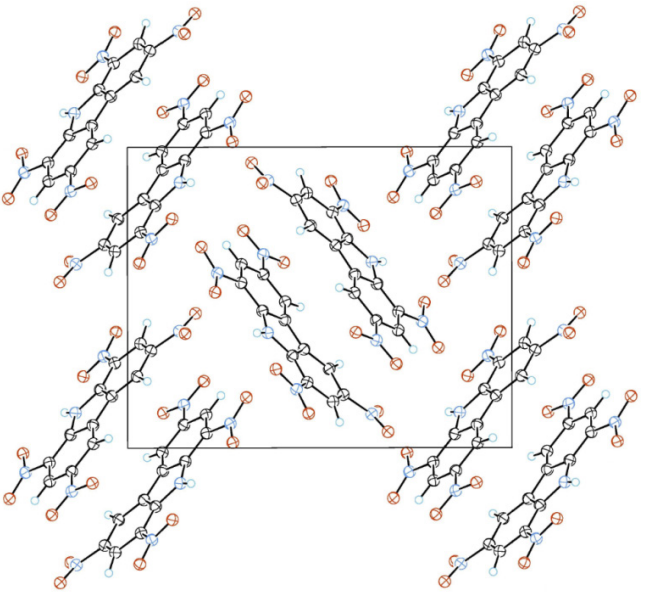

Figure 9. TNC crystal unit cell packing

3.5.3 General remarks on the crystal structure of TNC

The molecular structure of 1,3,6,8-TNC is notably intriguing. This molecule adopts an almost planar conformation, with relatively small dihedral angles throughout the nitrated heterocyclic framework. The largest dihedral angle, observed between the 3-nitro group and the carbazole core, is only 14.6°. The compound exhibits a comparatively high density; X-ray diffraction measurements at –100 °C indicated a density of 1.765 g/cm³, whereas the pycnometric density measured at room temperature (20 °C) was slightly lower, at approximately 1.73 g/cm³.

The increased density of TNC can be attributed to specific features of its molecular packing. The crystal structure reveals relatively strong π–π stacking interactions, which promote the formation of distinct molecular dimers. These dimers are evident in the crystal packing along the X-axis, as illustrated in Figure 9 (crystal unit cell projection).

The distance between parallel, superimposed molecular planes in the TNC crystal was 3.335 Å, while the shortest intermolecular atomic contact, specifically between atoms C-3 and C-7, was 3.73 Å, which is slightly shorter than the sum of their van der Waals radii. In addition to π–π stacking, hydrogen bonding is also present in the TNC crystal, notably both intramolecular NH···O hydrogen bonds and the less commonly observed intermolecular CH···O interactions were identified.

4 The Electron-accepting Ability and Quantum Mechanical Characteristics of TNC

As is characteristic of nitroaromatics, the electrochemical reduction of TNC proceeds irreversibly, exhibiting four distinct cathodic peaks with peak potentials (Ep *vs*. Ag/AgCl reference electrode, +0.205 V vs. NHE) at –170, –583, –687, and –806 mV. The peak currents were found to be diffusion-controlled, with a linear dependence on the square root of the scan rate over the range of 10 to 1000 mV/s. The first peak potential of TNC (–170 mV) is significantly more positive than that of tetryl (–300 mV) and even more so than that of TNT (–474 mV), both measured under identical experimental conditions as used for TNC.

The single-electron reduction potential (E^1_7) of nitro compounds is typically determined using pulse radiolysis techniques [53]. However, to the best of our knowledge, the E^1_7 value for TNC has not been experimentally established. A tentative E^1_7 ($E^1_{7(calc.)}$) for this compound has previously been estimated using an alternate approach, based on the linear correlation between the logarithm of the rate constants for flavoenzyme-mediated reduction of a broad range of nitroaromatic compounds including polynitroaromatic explosives, and their experimentally determined E^1_7 values [53]. This estimation yielded an $E^1_{7(calc.)}$ of –116 mV for TNC, which is close to that of tetryl (E^1_7(calc.) = –136 mV) and significantly higher than that of TNT (E^1_7 = –253 mV and $E^1_{7(calc.)}$ = –254 mV).

Alternatively, the electron-accepting capability, characterized by the LUMO energy (E_{LUMO} = –3.58 eV) and the global electrophilicity index ω = 3.84 eV, falls between those of tetryl (E_{LUMO} = –3.92 eV, ω = 3.84 eV) and TNT (E_{LUMO} = –3.46 eV, ω = 3.55 eV), as obtained at the same level of theory [9].

The regional electrophilicity and nucleophilicity of TNC, determined by the absolute LUMO density (|LUMO|) and the absolute HOMO density (|HOMO|) distributions, along with the most reactive atomic sites, identified by electrophilic (P_k^+) and nucleophilic (P_k^-) reactivity indices, are as shown in Figures 10(a) and 10(b), respectively. The most pronounced electrophilic sites are localized on the carbon atoms of the benzene rings at the ortho-positions with respect to the nitro groups (Figure 10(a)), whereas the most pronounced nucleophic site is localized on the –NH moiety of the fused pyrrole ring (Figure 10(b)), and the regional reactivity maps based on electrophilic and nucleophilic Parr function values, derived from atomic spin densities of the corresponding radical cation Figure 10(a) and anion radical Figure 10(b) species at the UB3LYP/cc-pVDZ level, using geometries optimized for the neutral form of the compound.

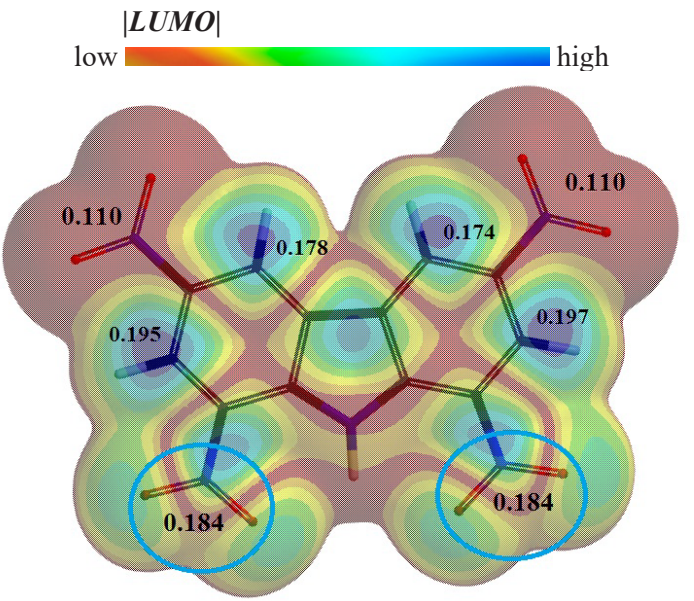

(a)

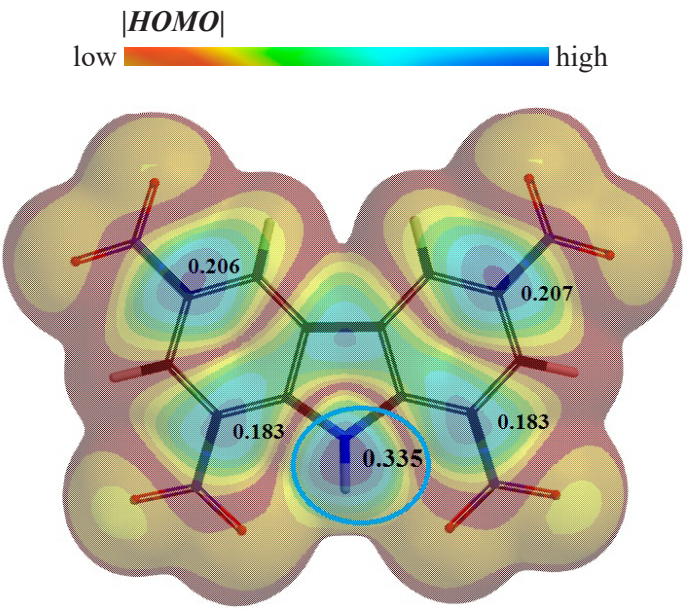

(b)

Figure 10. Absolute density maps of HOMO (a) and LUMO (b) of TNC (isovalue = 0.004 $Bohr^{-3/2}$)

Consistent with the redox behaviour of other nitroaromatic compounds, the nitro groups in TNC serve as the key redox-active centers, susceptible to reduction via single-electron or two-electron/hydride transfer pathways [9]. As shown in Figure 10(a), the nitro groups at the C-1 and C-8 positions display significantly higher P_k^+ function values compared to those at the C-3 and C-6, indicating a greater susceptibility to reduction at the C-1 and C-8 sites.

Aromatic high-energy compounds containing nitro groups exhibit distinct electrostatic potential (EP) distributions, primarily due to the strong electron-withdrawing nature of the nitro moieties. These groups exert both inductive and mesomeric effects, depleting electron density from the aromatic ring and contributing to the characteristic EP profiles observed in such compounds [54]. Figure 11 illustrates the EP map of TNC, projected onto the electron density isosurface at a value of 0.001 e/bohr³, superimposed with atomic partial charges, providing a detailed visualization of the electrostatic landscape.

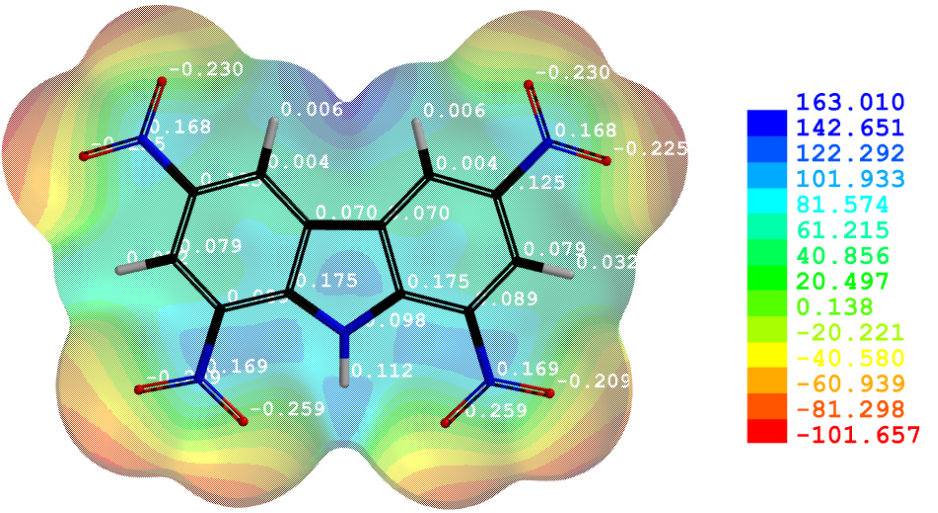

Figure 11. EP surface of TNC mapped onto the electron density isosurface (0.001 e/bohr³) in conjunction with atomic partial charges obtained at the RB3LYP/cc-pVDZ level; regions of maximum positive and negative EP are shown in dark blue and dark red, respectively; EP values are reported in kJ/mol

Negative EP regions are primarily localized along the molecular periphery, concentrated over the oxygen atoms of the nitro groups, with the most negative potentials reaching approximately –102 kJ/mol (*ca.* –1.05 eV). In contrast, positive EP regions are distributed across the carbazole core, with the most

electropositive areas observed near the –NH moiety, the C(5a)–C(4a) bond within the fused pyrrole ring, and the C(1a)–C(1) and C(8)–C(8a) bonds of the fused benzene rings, exhibiting potentials of up to ~163 kJ/mol (~1.70 eV). The partial charges, expressed as Mulliken charges localized on the nitro-groups at the C-1 and C-8 positions (Q_{NO2} = –0.302), were defined to be slightly more negative than those localized in positions of C-3 and C-6.

In addition, the electrostatic potential (EP) values at the midpoint of the C–NO_2 bonds at the C-1 and C-6 positions were approximately 108 kJ/mol (~1.12 eV), which are more positive than those observed for the corresponding bonds at the C-3 and C-6 positions (~85 kJ/mol or 0.88 eV).

One of the factors that may influence the mechanical sensitivity of energetic compounds is considered to be their global electronic hardness (η), commonly approximated by the LUMO-HOMO energy gap ($\eta = E_{LUMO} - E_{HOMO}$). Larger global hardness is roughly associated with greater molecular stability and/or reactivity [54-56]. Computational results show that TNC has a global hardness of 4.21 eV, identical to that of tetryl (η = 4.21 eV) and significantly lower than that of TNT (η = 4.99 eV) [9]. This suggests that, based on this parameter, TNC may exhibit mechanical sensitivity similar to that of tetryl.

5 Bond Dissociation Energies for NO_2 Cleavage in TNC

For energetic materials, the cleavage of certain „trigger“ bonds is widely recognized as a critical step in initiating explosive decomposition, with stability associated with the bond dissociation energy (BDE) [54, 57]. In polynitro compounds, the C–NO_2 and N–NO_2 bonds are typically identified as primary trigger bonds [54]. As described in the Experimental section, the BDE values for the C–NO_2 bonds in the TNC molecule were calculated using the B3LYP/6-31G(d) level of theory, which allowed a comparison of BDEs of TNC with those of other polynitroaromatics, whose BDEs have been assessed using the same computational methodology [57]. The BDE for the nitro group at the C-3 (or C-6) position of TNC was calculated as 66.87 kcal/mol (2.90 eV), slightly lower than that at the C-1 (or C-8) position, which was 68.37 kcal/mol (2.96 eV). These values imply that TNC may have a lower impact sensitivity than TNT, which has a reported BDE of 58.90 kcal/mol (2.55 eV), and potentially a comparable sensitivity to picramide (2,4,6-trinitroaniline, TNA), wth a BDE of 64.0 kcal/mol (2.80 eV) [57].

4 Conclusions

- 1,3,6,8-Tetranitrocarbazole (TNC, $C_{12}H_5N_5O_8$) is a high-energy nitro compound with applications in military pyrotechnic formulations. Therefore, optimizing its synthesis is of significant importance for improving performance and production efficiency [47, 58-61]. Our study compared two nitration methods for its synthesis:
  - Method A: potassium nitrate with oleum (H_2SO_4 with 20 % SO_3), and
  - Method B: fuming nitric acid with oleum.

  Method A was found to be the more efficient and more selective procedure, affording a higher yield (62%) and greater product purity compared to Method B (58%).
- For the first time, it was observed that nitration of carbazole *via* Method B leads to the formation of a minor by-product, trinitrocarbazole sulfonic acid ($C_{12}H_6N_4O_9S$, MW = 382), in 2-5% yield. HPLC–MS analysis confirmed the absence of the isomeric 1,2,6,8-TNC, previously reported by Murphy *et al.* [52], among the reaction products, even at trace levels.
- A single crystal of pure 1,3,6,8-TNC was grown from a nitromethane solution and used for detailed X-ray crystallographic analysis. The compound crystallizes in the monoclinic system, space group $P2_1/c$. The calculated crystal density at –100 °C is 1.765 g/cm³, while the density measured by pycnometry at 20 °C is 1.73 g/cm³. Notably, this density exceeds that of TNT (1.654 g/cm³), highlighting the potential of TNC as a high-density energetic material.
- The main properties of 1,3,6,8-TNC are as follows:
  - molecular weight: 347.21 g/mol,
  - melting point: 296 °C,
  - flash point: 350 °C,
  - maximum solubility in water: 20-30 × 10^{-6} mol/L,
  - heat of formation: –18.9 kJ/mol,
  - oxygen balance to CO_2: –85.2%, and
  - density at room temperature: 1.73 g/cm³.

  The relative explosive power (brisance) of TNC compared to TNT is approximately 86-95%, depending on the test method employed [62].
- The electron-accepting ability and quantum mechanical properties of TNC closely resemble those of tetryl. However, based on the calculated C–NO_2 bond dissociation energies, TNC is predicted to exhibit lower sensitivity than both tetryl and TNT, and similar sensitivity to picramide (2,4,6-trinitroaniline). Consequently, the overall explosive properties of TNC are expected to be close to those of TNT and picramide.

References

[1] Collin, G.; Hooke, H. Carbazole. In: *Ullmann's Encyclopedia of Industrial Chemistry*, 5th Ed., (Gerhartz, W., Ed.), New York, **1986**, p. 59; https://doi.org/10.1002/14356007.a05_059.pub2.

[2] Graebe, C.; Glaser, C. Ueber Carbazol. *Justus Liebigs Ann. Chem.* **1872**, *163*: 343-360.

[3] Wang, Y.; Zhang, W.; Wang, D.; Ma, R.; Ai, L.; Xu, M.; Jia, D.; Guo, N.; Wang, L.; Meng, L. Highly Efficient Separation of Anthracene and Carbazole in Crude Anthracene by Composite Extractants with Low Viscosity. *Chem. Eng. J.* **2025**, *510* paper 161589; https://doi.org/10.1016/j.cej.2025.161589.

[4] Chen, Y.F.; Zong, Z.M.; Li, X.K.; Liu, G.H.; Yang, Z.; Jiang, X.G.; Liu, F.J.; Wei, X.Y.; Guo, Q.J.; Zhao, T.S.; Bai, H.C.;Wang, B.J. An Effective Approach for Separating Carbazole and Its Derivates from Coal-Tar-derived Anthracene Oil using Ionic Liquids. *Energy Fuels* **2018**, *33*: 513-522; https://doi.org/10.1021/acs.energyfuels.8b02675.

[5] Xu, Z.; Wu, D.; Fang, C.; Li, Y. Mini-review on the Novel Synthesis and Potential Applications of Carbazole and Its Derivatives. *Des. Monomers Polym.* **2023**, *26*: 90-105; https://doi.org/10.1080/15685551.2023.2194174.

[6] Higginbotham, H.; Karon, K.; Ledwon, P.; Data, P. Carbazoles in Optoelectronic Applications. *Display and Imaging* **2017**, *2*: 207-216.

[7] Alothman, S.; Kandil, F.; Deep, A. Carbazole Derivatives as Antioxidant and Anticorrosion Materials. *Results Chem.* **2024**, *9* paper 101667; https://doi.org/10.1016/j.rechem.2024.101667.

[8] Zhang, F.F.; Gan, L.L.; Zhou, C.H. Synthesis, Antibacterial and Antifungal Activities of Some Carbazole Derivatives. *Bioorg. Med. Chem. Lett.* **2010**, *20*: 1881-1884; https://doi.org/10.1016/j.bmcl.2010.01.159.

[9] Šarlauskas, J.; Polmickaitė-Smirnova, E.; Čėnas, N.; Krikštopaitis, K.; Anusevičius, Ž. The QSAR Study for Antibacterial Activity of Structurally Diverse Nitroaromatics. *Chemija* **2019**, *30*: 41-48; https://doi.org/10.6001/chemija.v30i1.3924.

[10] Patil, S.A.; Patil, Sh.A.; Ble-González, E.A.; Isbel, S.R.; Hampton, S.M.; Bugarin, A. Carbazole Derivatives as Potential Antimicrobial Agents. *Molecules* **2022**, *27*: 6575; https://doi.org/10.3390/molecules27196575.

[11] Sellamuthu, S.; Gutti, G.; Kumar, D.; Kumar Singh, S. Carbazole: A Potent Scaffold for Antitubercular Drugs. *Mini-Rev. Org. Chem.* **2018**, *15*: 498-507; https://doi.org/10.2174/1570193X15666180220141342.

[12] Tiwari, A.; Bendi, A.; Bhathiwal, A.S. Carbazoles and Their Derivatives as Anti-inflammatory Agents. In *Heterocyclic Anti-Inflammatory Agents: A Guide for Medicinal Chemists.* Bentham Science Publishers, UAE, Sharjah, **2024**, pp. 144-163; https://doi.org/10.2174/9789815223460124010 1.

[13] Ceramella, J.; Rosano, C.; Iacopetta, D.; Ben Toumia, I.; Chekir-Ghedira, L.; Maatouk, M.; Mariconda, A.; Longo, P.; Dallemagne, P.; Rochais, C.; Sinicropi,

M.S. Anti-Breast Cancer Properties and *In Vivo* Safety Profile of a Bis-Carbazole Derivative. *Pharmaceutics **2025**, 17*(3) paper 415; https://doi.org/10.3390/pharmaceutics17040415.

[14] Waghmare, P.S.; Chabukswar, A.R.; Raut, K.G.; Giri, P.T. A Review on Carbazole and Its Derivatives as Anticancer Agents from 2013 to 2024. *Chirality* **2025**, *37* paper e70021; https://doi.org/10.1002/chir.70021.

[15] Zhang, H.; Zhang, W.; Zhu, M.; Awadasseid, A. A Review on the Anticancer Activity of Carbazole-based Tricyclic Compounds. *Curr. Med. Chem.* **2024**, *31*: 4826-4849; https://doi.org/10.2174/0929867331666230825104254.

[16] *Carbazole: N-Ethylcarbazole, N-Vinylcarbazole, 1,3,6,8-Tetranitrocarbazole, 1,8-Dichloro-3,6-dinitrocarbazole.* (Martin, H., Ed.), Livres Groupe, Books LLC, Fort Lauderdale, Florida, USA **2010**, pp. 1-22; ISBN-13: 9781159635589.

[17] Rahimi-Nasrabadi, M.; Zahedi, M.M.; Pourmortazavi, S.M.; Heydari, R.; Rai, H.; Jazayeri, J.; Javidan, A. Simultaneous Determination of Carbazole-based Explosives in Environmental Waters by Dispersive Liquid-Liquid Microextraction Coupled to HPLC with UV-Vis Detection. *Mikrochim. Acta* **2012**, *177*: 145-152; https://doi.org/10.1007/s00604-012-0762-0.

[18] Pourmortazavi, S.M.; Rahimi-Nasrabadi, M.; Rai, H.; Besharati-Seidani, A.; Javidan, A. Role of Metal Oxide Nanomaterials on Thermal Stability of 1,3,6-Trinitrocarbazole. *Propellants Explos. Pyrotech.* **2016**, *41*(5): 912-918; https://doi.org/10.1002/prep.201500312.

[19] Farahani, H.; Rahimi-Nasrabadi, M. Trace Determination of Tetranitrocarbazole in Aquatic Environment Using Carbon Dot-Dispersive Liquid-Liquid Microextraction Followed by UV-Vis Spectrophotometry. *Iranian J. Anal. Chem.* **2018**, *5*: 17-24; https://ijac.journals.pnu.ac.ir/article_4488_d0d6678875a5d70ce77b6501c336b05b.pdf?lang=fa (Accessed at 15-06-2025).

[20] Urbanski, T. *Chemistry and Technology of Explosives.* Warszawa, PWN, **1964**, Vol. 1, pp. 566-569.

[21] Meyer, R.; Köhler, J.; Homburg, A. *Explosives.* 7th Ed., Weinheim, Germany, **2016**, p. 313; ISBN: 978-3-527-68961-3.

[22] Fedoroff, B.T. *Dictionary of Explosives, Ammunition and Weapons (German Section).* Picatinny Arsenal Technical Report No. 2510, Dover, New Jersey, US, **1958**.

[23] Fatah, A.A.; Arcilesi, Jr., R.D.; McClintock, J.A.; Lattin, C.H.; Helinski, M.; Hutchings, M. *Guide for the Selection of Explosives Detection and Blast Mitigation Equipment for Emergency First Responders.* Preparedness Directorate Office of Grants and Training, Guide 105–07, H-6. Washington, DC, US, Feb. **2008**, pp. 1-364; https://www.nist.gov/system/files/documents/oles/105-07_32812-ExploxivesGuideFinal5-12-08.pdf.

[24] *Technical Manual TM 9-1300-214, Military Explosives.* Department of the Army, Washington, DC, US, **1984**.

[25] *Technical Manual TM 9-1300-200, Ammunition, General*. Department of the Army, Washington, DC, US, **1969**.

[26] Agrawal, J.P.; Hodgson, R. *Organic Chemistry of Explosives.* Wiley Intersci., New York, US, pp. 195-203, **2007**; ISBN: 978-0-470-02967-1.
[27] Agrawal, J.P. *High Energy Materials. Propellants, Explosives and Pyrotechnics*. Wiley-WCH Verlag GmbH&Co, KGaA, Weinheim, **2010**; ISBN: 978-3-527-32610-5.
[28] *High Energy Density Materials (Structure and Bonding).* (Klapötke, T.M., Ed.), Springer, Berlin/Heidelberg, **2007**, pp. 1-286; ISBN 13: 9783540722014.
[29] *Explosives-Booster.* **2014**, http://www.globalsecurity.org/military/systems/munitions/explosives-booster.htm (Accessed at 07-02-2025).
[30] Akhavan, J. Introduction to Propellants and Pyrotechnics. In: *The Chemistry of Explosives*. 2nd Ed., Cambridge, UK, RSC, **2004**, pp. 149-164; ISBN: 978-1-84755-202-0.
[31] Pourmortazavi, S.M.; Rahimi-Nasrabadi, M.; Rai, H.; Jabbarzadeh, Y.; Javidan, A. Effect of Nanomaterials on Thermal Stability of 1,3,6,8-Tetranitrocarbazole. *Cent. Eur. J. Energetic Mater.* **2017**, *14*: 201-216; https://doi.org/10.22211/cejem/65140.
[32] Voigt, Jr., H.W. *Impact Resistant Pressable Explosive Composition of High Energetic Material Content.* US Patent 4,251,301, **1981**.
[33] Geerlings, P.; De Proft, F. Chemical Reactivity as Described by Quantum Mechanical Methods. *Int. J. Mol. Sci.* **2002**, *3*: 276-309; https://doi.org/10.3390/i3040276.
[34] Domingo, L.R.; Perez, P.; Saez, J.A. Applications of the Conceptual Density Functional Theory Indices to Organic Chemistry Reactivity. *Molecules* **2016**, *21*: 748-769; https://doi.org/10.3390/molecules21060748.
[35] Domingo, L.R.; Perez, P.; Saez, J.A. Understanding the Local Reactivity in Polar Organic Reactions through Electrophilic and Nucleophilic Parr Functions. *RCS Adv.* **2013**, *3*: 1486-1494; https://doi.org/10.1039/C2RA22886F.
[36] Rice, B.M.; Sahu, S.; Owens, F.J. Density Functional Calculations of Bond Dissocation Energies for NO_2 Scission in Some Nitroaromatic Molecules. *J. Mol. Struct. (THEOCHEM)* **2002**, *583*: 69-72; https://doi.org/10.1016/S0166-1280(01)00782-5.
[37] Kyziol, J.B.; Daszkiewicz, Z. Nitration in the Carbazole Series. *Tetrahedron* **1984**, *40*: 1857-1861; https://doi.org/10.1016/S0040-4020(01)91140-8.
[38] Ziersch, P. Ueber einige Carbazolderivate. *Berichte der deutschen chemischen Gesellschaft* **1909**, *42*: 3797-3800.
[39] Chakrabarty, M.; Batabyal, A. A New Method of Nitration of Carbazoles using Ceric Ammonium Nitrate (CAN). *Synth. Commun.* **1994**, *24*: 1-10; https://doi.org/10.1080/00397919408012618.
[40] Lancelot, J.C.; Gazengel, J.M.; Robba, M. Ètude des reactions de nitration de l'acetamido-3 ethyl-9 carbazole. *J. Het. Chem.* **1981**, *18*: 1281-1285; https://doi.org/10.1002/jhet.557018070.
[41] Ledochowski, A.; Zirra, J. Research on Tumor Inhibiting Compounds. 54. Syntheses of N-9-substituted 1-Nitrocarbazoles, 2-Nitrocarbazoles, 3-Nitrocarbazoles, 4-Nitrocarbazoles, and 5-Nitro-1,2,3,4-tetrahydrocarbazoles or 7-Nitro-1,2,3,4-

tetrahydrocarbazoles. *Rocz. Chem.* **1975**, *49*: 1179-1182.
[42] Kyziol, J.B.; Daszkiewicz, Z. Nitration in the Carbazole Series, II. *Liebigs Ann. Chem.* **1985**, *7*: 1336-1345; https://doi.org/10.1002/jlac.198519850705.
[43] Holloway, T.C.; Ball, L.M. Synthesis and Mutagenicity of a Series of Nitrated Carbazoles and Hydroxycarbazoles. *Mutagenesis* **1993**, *8*: 321-327; https://doi.org/10.1093/mutage/8.4.321.
[44] Nagarajan, R.; Muralidharan, D.; Perumal, P.T. A New and Facile Method for the Synthesis of Nitrocarbazoles by Urea Nitrate. *Synth. Commun.* **2004**, *34*: 1259-1264; https://doi.org/10.1081/SCC-120030313.
[45] Kyziol, J.B.; Domanski, A. An Improved Synthesis of 2-Aminocarbazole. *Org. Prep. Proced. Int.* **1981**, *13*: 419-421; https://doi.org/10.1080/00304948109356154.
[46] Kyzioł, J.B.; Daszkiewicz, Z.; Hetper, J. Fragmentation of Some Nitrocarbazoles and Their 9-Alkyl Derivatives. *Org. Mass Spectrom.* **1987**, *22*: 39-42; https://doi.org/10.1002/oms.1210220110.
[47] Christofi, J.M.B. *Synthesis of Aromatic Polynitro Compounds.* PhD Thesis, London College University, UK, **1994**, pp. 153-161; https://www.proquest.com/openview/1ee68220ba54f718f7cc9b937af824fc/1?cbl=2026366&diss=y&pq-origsite=gscholar&parentSessionId=OKzyk9KRStTsLaJNvetFSJSINmswCDzG85JUYWdJjOc%3D (Accessed at: 08.02.2025).
[48] Shufen, Z.; Danhong, Z.; Jinzong, Y. Nitration of Carbazole and N-Alkylcarbazoles. *Dyes Pigm.* **1995**, *27*: 287-296; https://doi.org/10.1016/0143-7208(94)00054-6.
[49] *The Chemistry of Amino Nitroso and Nitro Compounds and Their Derivatives, Supplement F, Part 1*. (Patai, S., Ed.) Wiley, Chichester, **1982**, Vol. 29, p. 319.
[50] Iles, D.H.; Ledwith, A. Charge Transfer Spectra and Reaction Intermediates: Photochemical Nitration of Carbazoles with Tetranitromethane. *J. Chem. Soc. D* **1969**: 364-365.
[51] Šarlauskas, J.; Anusevičius, Ž.; Stankevičiūtė, J.; Krikštopaitis, K.; Misevičienė, L.; Čėnas, N.; Miliukienė, V.; Bružaitė, G.; Laurynėnas, A. Nitrocarbazoles: Studies on Their Electron Accepting Properties, Enzymatic Reactivity and Cytotoxicity. *Proc. Semin. New Trends Res. Energ. Mater.*, Pardubice Czech Republic, **2015**, 780-788.
[52] Murphy, D.B.; Schwartz, F.R.; Picard, J.P.; Kaufman, J.V.R. Identification of Isomers Formed in the Nitration of Carbazole. *J. Am. Chem. Soc.* **1953**, *75*: 4289-4291; https://doi.org/10.1021/ja01113a042.
[53] Šarlauskas, J.; Nivinskas, H.; Anusevičius, Ž.; Misevičienė, L.; Marozienė, A.; Čėnas, N. Estimation of Single-Electron Reduction Potentials (E^1_7) of Nitroaromatic Compounds according to the Kinetics of Their Single-Electron Reduction by Flavoenzymes. *Chemija* **2006**, *17*(1): 31-37.
[54] Guo, J.; Lin, G.; Peng, X. Density Functional Theory (DFT) Study on the Structures and Energy Properties of High Energy Density Materials Based on Polynitroazofurazan Derivatives. *Mater. Today Commun.* **2024**, *40* paper 109759; https://doi.org/10.1016/j.mtcomm.2024.109759.
[55] Geerlings, P.; De Proft, F. Chemical Reactivity as Described by Quantum Mechanica

Methods. *Int. J. Mol. Sci.* **2002**, *3*: 276-309; https://doi.org/10.3390/i3040276.
[56] Domingo, L.R.; Perez, P.; Saez, J.A. Applications of the Conceptual Density Functional Theory Indices to Organic Chemistry Reactivity. *Molecules* **2016**, *21*: 748-769; https://doi.org/10.3390/molecules21060748.
[57] Rice, B.M.; Sahu, S.; Owens, F.J. Density Functional Calculations of Bond Dissocation Energies for NO_2 Scission in Some Nitroaromatic Molecules. *J. Mol. Struct. (THEOCHEM)* **2002**, 583: 69-72.
[58] Singh, S.K.; Price, D.W. 1,3,6,8-Tetranitrocarbazole (TNC): Synthesis and Optimization. *Technical Report ARMET-TR-12014*, Picatinny Arsenal, New Jersey, US **2013**.
[59] Hedberg, M.E.; Wickiam, J.A. *Military Explosives.* Department of the Army Technical Manual TM 9-1300-214, Washington, DC, **1985**.
[60] Cooper, P.W.; Kurowski, S.R. *Introduction to the Technology of Explosives.* John Wiley & Sons, Hoboken/New Jersey, US, **1997**; ISBN: 978-0-471-18635-9.
[61] Christofi, J. *A New and Improved Methods to Production of Energy Rich Materials.* Naval Weapons Support Center, Report AD-A231 256, **1990**; https://citeseerx.ist.psu.edu/document?repid=rep1&type=pdf&doi=1540caac2d3d828c4bce614cd998b38a4e33a4c8 (Accessed at 06-02-2025).
[62] Fedoroff, B.T.; Sheffield, O.E. *Encyclopedia of Explosives and Related Items (PART 2700).* Picatinny Arsenal, New Jersy, US, **1962**, Vol. 2, p. B 289.

Authorship contribution statement

Jonas Šarlauskas: conception, methods, performing the experimental part
Mantas Jonušis: methods, performing the experimental part
Simona Jonušienė: performing the experimental part
Narimantas Čėnas: foundations, other contribution to the publication
Kastis Krikštopaitis: methods, performing the experimental part
Jonita Stankevičiūtė: performing the experimental part
Žilvinas Anusevičius: methods, performing the statistical analysis, other contribution to the publication

Submitted: June 19, 2025
Revised: December 19, 2025
First published online: December 30, 2025